



## THE EFFECT OF THROUGH-THICKNESS CRACKS ON THE BALLISTIC PERFORMANCE OF CERAMIC ARMOUR SYSTEMS

I. HORSFALL and D. BUCKLEY

Cranfield University, RMCS Shrivenham, Swindon, Wiltshire SN6 8LA, U.K.

(Received 9 March 1995; in revised form 11 May 1995)

**Summary**—Full width through-thickness cracks were introduced into the ceramic tiles of ceramic faced composite armour panels. The ballistic limit velocity for projectiles striking directly on the crack was measured and compared with undamaged panels. The effect of the cracks was to lower the  $V_{50}$  ballistic limit velocity to  $744 \text{ m s}^{-1}$  compared to  $764 \text{ m s}^{-1}$  for undamaged panels, a drop of only 3%. This means that the presence of cracks in a ceramic armour tile should not be sufficient reason to require replacement of the panel, a fact of some importance given the likelihood of damage in the military environment. It is proposed that the small value of the reduction in performance is observed because the cracked ceramic is still effectively confined by the presence of a well bonded composite backing and a frontal spall shield. The presence of a large crack at the impact point has little effect as the ceramic in this area is anyway extensively comminuted ahead of the projectile upon impact. The backing and spall shield conserve the structural integrity of the panel and this acts to contain the radial stresses generated by the impact event. The performance of the armour system has also been assessed by measurement of the  $V_0$  ballistic limit velocity determined from residual momentum of penetrating projectiles and armour fragments. The standard panels showed a  $V_0$  of  $743 \text{ m s}^{-1}$  compared to  $699 \text{ m s}^{-1}$  for the pre-cracked panels.

### NOTATION

$V_{50}$  initial projectile velocity for which there is a 50% probability of penetration  
 $V_0$  initial projectile velocity for which there is a 0% probability of penetration

### 1. INTRODUCTION

Complex armour systems, consisting of a hard front face of ceramic and an energy absorbing rear face of polymer composite or aluminium alloy, are widely used in ballistic armour applications on vehicles, aircraft and personnel. A perceived disadvantage of such systems is the brittle nature of the ceramic facing which is shattered during ballistic impact or can be cracked during rough handling. This would be expected to limit the performance of the systems if multiple ballistic impacts were experienced or if prior handling damage had occurred. The aim of this paper is to show the effect of such cracks in the ceramic layer upon the ballistic performance of the armour system. These cracks are representative of radial cracks caused by ballistic impacts or damage from in-service handling.

The failure mechanisms of ceramic faced armour subject to high velocity impact have been widely studied [1–4], the process is represented in Fig. 1. On impact, a metallic projectile is deformed due to the relatively high compressive strength of the ceramic so that some blunting takes place. Under the impact point the stresses are mainly compressive and therefore the ceramic will initially deform in an elastic manner. Radial tensile stresses are generated on the front surface of the ceramic which lead to the formation of one or more Hertzian cracks. These cracks start as circular cracks normal to the surface at the periphery of the contact patch. They then propagate into the ceramic at  $15\text{--}65^\circ$  to the surface in mode II (shear). If the penetrator has sufficient energy and is sufficiently hard then it is subsequently possible to exceed the compressive strength of the ceramic leading to comminution of the material in front of the penetrator. Elastic waves produced by the initial impact will reflect from the rear surface and edges of the ceramic tile as tensile waves and may cause additional fracturing. This effect might be enhanced if the backing material is of a low acoustic impedance as in the case for most polymeric composites. Flexing of the backing layer and ceramic lead to

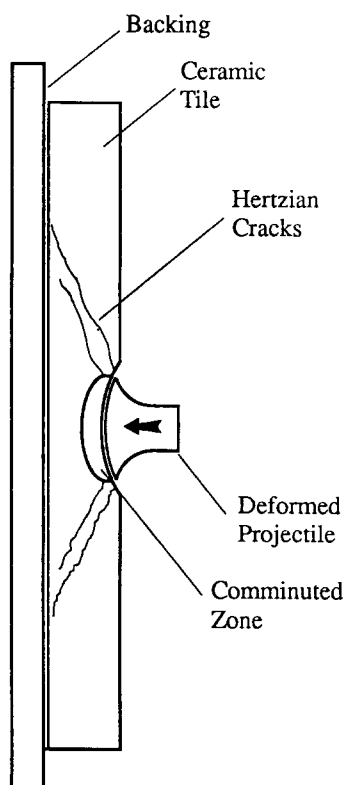


Fig. 1. A representation of the deformation of the target and projectile during ballistic impact.

the formation of radial cracks which spread out from the impact point towards the edges of the ceramic tile. The kinetic energy of the projectile is dissipated by deformation and damage mechanisms within the backing material. The main purpose of the ceramic is to spread this the kinetic energy over a large area of the backing via the Hertzian conoid, and to erode the projectile. It has been shown [4] that little energy is dissipated by fracture of the ceramic.

The conoid of ceramic at the impact point is usually seen to be extensively fractured but is often retained on the backing layer by the adhesive used to bond the two layers. It has been suggested [1] that radial fracture of the ceramic must be delayed in order to obtain optimum armour performance, however this conclusion is based on high speed photographic observations only, and it is possible that premature cracking is only an indication of poor support or poor mechanical properties in the ceramic. Recent work [2] has shown that extensive cracking takes place within the conoid producing a granular rubble which supports the load imposed by the projectile. Confinement of this rubble by the surrounding material makes it an effective barrier to penetration and it has been shown that the resistance of this material to flow by inter-particle sliding is an important factor in the effectiveness of the armour. It has been suggested [5] that expansion of this rubble as it fractures generates radial tensile stresses which then cause radial cracking.

If there is a pre-existing large crack in the ceramic in the impact area then it might be expected to reduce the performance of the armour. The unconfined material at the fracture surfaces would fail prematurely under a compressive load and comminuted material could flow into the crack allowing premature compressive collapse. Additionally the stiffness of the armour structure might be reduced, leading to increased radial cracking due to bending of the armour panel. In current ceramic faced systems [6] it is usual to use a high strength adhesive to bond the ceramic to the backing material. It is also usual to apply a spall shield consisting of a single laminate of polymer composite to the front face of the ceramic. The combined effect of the backing and spall shield is to confine the ceramic tile even if it has been

shattered or broken. Cracks in the ceramic tile will tend to remain closed and except for the area within a few calibres of the impact site the panel should retain its structural integrity after ballistic impact. Large through-thickness cracks are prevented from opening so that the material on the crack surface is effectively constrained by the material on the opposite crack surface. The effect of the backing and spall shield is to tie the surfaces together so that radial constraint is still present should a projectile strike the crack. Therefore the effect of a through-thickness crack in the ceramic layer upon the ballistic performance of the armour system should be negligible.

This paper describes a series of ballistic tests on alumina/GRP target panels in which the performance of a standard panel is compared to that of a pre-cracked panel. The pre-cracked panels had a single through-thickness crack introduced onto which the ballistic impact was performed. The impact was placed such that the crack would be directly under the impact site. The crack was representative of a radial crack from a previous ballistic impact or a crack introduced by rough handling or accidental damage.

## 2. EXPERIMENTAL METHODS

### 2.1. Target panels

Alumina tiles (grade FA) of 6 mm thickness and measuring  $100 \times 100$  mm were obtained from Morgan Matroc Ltd. These were bonded to 9 mm thick E-glass composite panels, supplied by T & N Technology Ltd, using Sikaflex 221 adhesive. The adhesive was applied as a thin layer between the tile and backing, and was also used to provide a bead around the tile to produce additional lateral containment. The properties of each of the three components are listed in Table 1 and the target construction is shown diagrammatically in Fig. 2. Half of the panels were used in this configuration with a single layer of woven fibreglass bonded to the front surface using polyester resin. The other set of panels had a single through-thickness crack introduced. This was produced by scribing the surface of the tile after it had been bonded to the backing. The panel was then loaded in three-point bending to produce a single through-thickness crack centrally across the entire tile. The crack was marked with dye penetrant and then a single layer of fibreglass was bonded to the front surface.

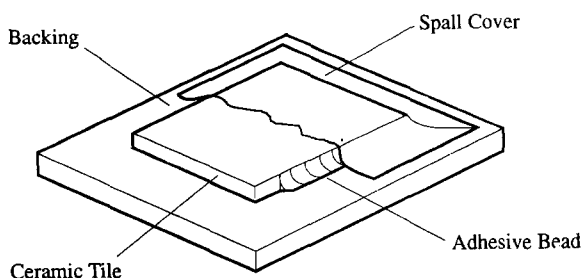


Fig. 2. Configuration of the target panels.

Table 1. Component parts of the armour panels

	<i>Alumina FA</i>	<i>E-glass composite</i>	<i>Sikaflex 221</i>
Size (mm)	100 × 100	150 × 150	
Thickness (mm)	6	9 (17 ply plain weave)	1 (approx.)
Composition	95% Al <sub>2</sub> O <sub>3</sub>	27% chlorinated polyester resin	polyurethane
Density kg m <sup>-3</sup>	3680	2100	
Tensile strength (MPa)	350 (MoR)	15.8	1.8
Elongation to failure (%)			450

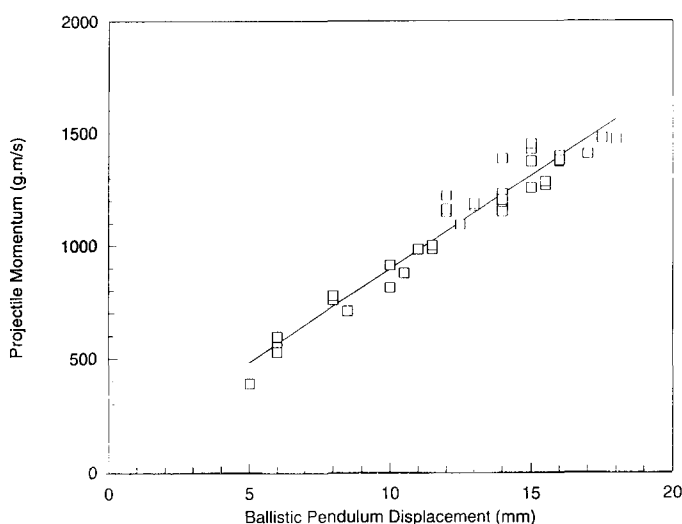


Fig. 3. Calibration plot for the ballistic pendulum.

## 2.2. Range equipment

The NATO standard  $7.62 \times 51$  mm armour piercing round (Fabrique Nationale, P80) was used as the ballistic threat. This has a total mass of 9.75 g and contains a 3.8 g hardened steel penetrator with a Vickers hardness of 870. The round was fired from a proof housing at a range of 10 m from the target panels. A laser designator was used to achieve accurate aiming and velocity was measured by optical gates placed 2 m and 6 m from the target. Paper screens were placed in the projectile's line of flight to check for yaw. Projectile velocity was adjusted by varying the charge in the cartridge case. The panels were rigidly clamped around their periphery in a steel frame.

A 24 kg ballistic pendulum was placed behind the target to allow an assessment of residual energy on perforated panels. This was calibrated by firing Browning .32 calibre pistol rounds at low velocities. The calibration plot is shown in Fig. 3, in which it can be seen that a good linear fit is achieved if the velocity of the projectile is plotted against the momentum recorded by the pendulum. An initial assessment of ballistic limit velocity was obtained from the residual momentum of perforating projectiles measured from the ballistic pendulum. A straight line was fitted to a plot of strike velocity vs residual momentum the intercept with the velocity axis being an estimation of the  $V_0$  ballistic limit velocity. This follows a procedure similar to that described by Tobin [7]. Further tests then used various velocities giving both full and partial penetration in order to determine the  $V_{50}$  ballistic limit velocity as defined in NATO Stanag 2920 [8].

## 3. RESULTS

### 3.1. Ballistic tests

A single round was fired into each test panel of the standard and pre-cracked types. Initially several high velocity tests were performed so that the ballistic limit velocity could be estimated from the residual momentum measured by the ballistic pendulum. Table 2 lists the results used in the calculation of ballistic limit velocities for the standard and pre-cracked tiles, the distance of the centre of the strike point from the pre-crack is also tabulated. Figures 4 and 5 show the residual energy as a function of impact velocity for all the tests.

The ballistic limit velocity can be estimated by extrapolation of a line joining these points to produce a  $V_0$  ballistic limit. A linear extrapolation was used as the range of velocities was small and only a few data points were used. The  $V_0$  was estimated as  $743 \pm 17 \text{ m s}^{-1}$  for the standard panels and  $699 \pm 10 \text{ m s}^{-1}$  for the pre-cracked panels. It can be seen that there is considerable variability in the test results such that the highest velocity producing partial

Table 2. Ballistic test results for standard and pre-cracked panels

Standard tiles		Cracked tiles		
Velocity ( $\text{m s}^{-1}$ )	Residual energy ( $\text{g m s}^{-1}$ )	Velocity ( $\text{m s}^{-1}$ )	Residual energy ( $\text{g m s}^{-1}$ )	Distance from pre-crack (mm)
703	0	703	0	0
724	0	705	0	5
747	0	720	1400	3
753	1180	722	0	0
754	1550	723	0	5
764	1450	733	2700	5
767	0	734	0	5
769	0	735	0	3
771	550	743	2500	0
780	0	746	0	0
802	2600	747	0	4
		753	3400	3
		756	0	5
		762	0	5
		772	3500	5
		773	4950	0

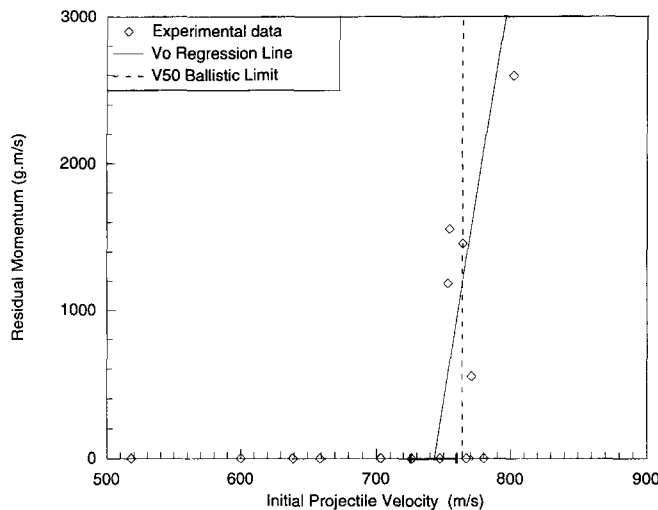


Fig. 4. Ballistic test results for the standard panels, showing all data points, the linear regression analysis for  $V_0$  including error bars, and the calculated  $V_{50}$ .

penetration is considerably greater than the lowest velocity producing full penetration. This scatter is greater for the pre-cracked tiles as might be expected due to the addition of a further variable. The  $V_{50}$  ballistic limit velocity was calculated according to the procedure of NATO Stanag 2920 [8]. This dictates that the limit velocity is the mean of 6 shots, the three highest velocities producing partial penetration and 3 lowest velocities producing full penetration. These 6 velocities must lie within a range of  $40 \text{ m s}^{-1}$ . If the range of velocities is greater then the average is taken over 10 shots, which must then be within a range of  $50 \text{ m s}^{-1}$ . This calculation has been performed using the data for the standard and pre-cracked targets for means of 6, 8 and 10 shots. This has been repeated for the pre-cracked panels with all data for shots landing 5 mm or greater from the crack being discounted. The results of these calculations are shown in Table 3.

For the standard panel the average calculated over 6 shots is  $764 \text{ m s}^{-1}$  and is within the allowed range. For the pre-cracked panels the average for all groups is marginally outside the range limits and is approximately  $745 \text{ m s}^{-1}$ . If only data for shots close to the pre-crack is used then the  $V_{50}$  over 6 shots is  $740 \text{ m s}^{-1}$  and is within the range limits. Therefore it can be

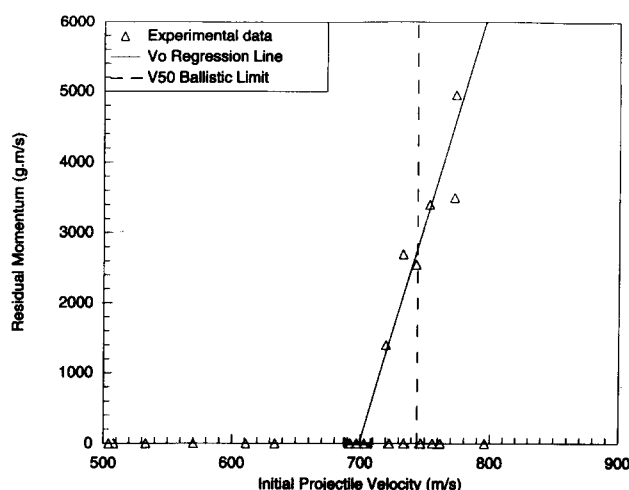


Fig. 5. Ballistic test results for the pre-cracked panels, showing all data points, the linear regression analysis for  $V_0$  including error bars, and the calculated  $V_{50}$ .

Table 3.  $V_{50}$  Ballistic limit velocities

Standard panels			Pre-cracked panels—all panels		Pre-cracked panels less than 5 mm from crack	
Designation	Range	$V_{50}$	Range	$V_{50}$	Range	$V_{50}$
Over 6 shots	27	765	42	743	33	741
Over 8 shots	33	763	42	745	51	742
Over 10 shots	76	763	52	747		

seen that the introduction of a full width, through-thickness, pre-crack reduces the  $V_{50}$  ballistic limit velocity from  $764 \text{ m s}^{-1}$  to  $740 \text{ m s}^{-1}$ , a drop of 3%.

### 3.2. Examination of target panels

Following the ballistic tests, the spall shields were carefully removed to expose the fragments of the ceramic tiles. For the standard panels the fracture appearance was as depicted in Fig. 6. The calibration plot is shown in Fig. 3. The region around the impact site was reduced to fine fragments, between 10 and 12 radial cracks were observed and typically 2 circumferential cracks. Although the circumferential cracks occur at an almost constant diameter from the impact site they are disjointed across the radial cracks indicating that the radial cracks are formed first.

In the pre-cracked panels the geometry of the cracking depended upon the position of the impact site. If the impact site was within one projectile radius of the pre-crack then the appearance was similar to the standard panels. However when the point of impact was further from the pre-crack then a different pattern was observed in which the damage was largely confined to the portion of the ceramic tile struck by the projectile. In both cases the number of radial cracks was between 8 and 12. Figures 7 and 8 show the appearance of pre-cracked tiles struck adjacent to and coincident with the pre-crack.

## 4. DISCUSSION

### 4.1. Measurement of ballistic limit velocity

The  $V_{50}$  ballistic limit velocity has been used as the primary measure of performance for comparison of the standard and pre-cracked panels as it is a widely accepted measure of armour performance. As only 6 velocities were used to determine the  $V_{50}$  it is necessary to

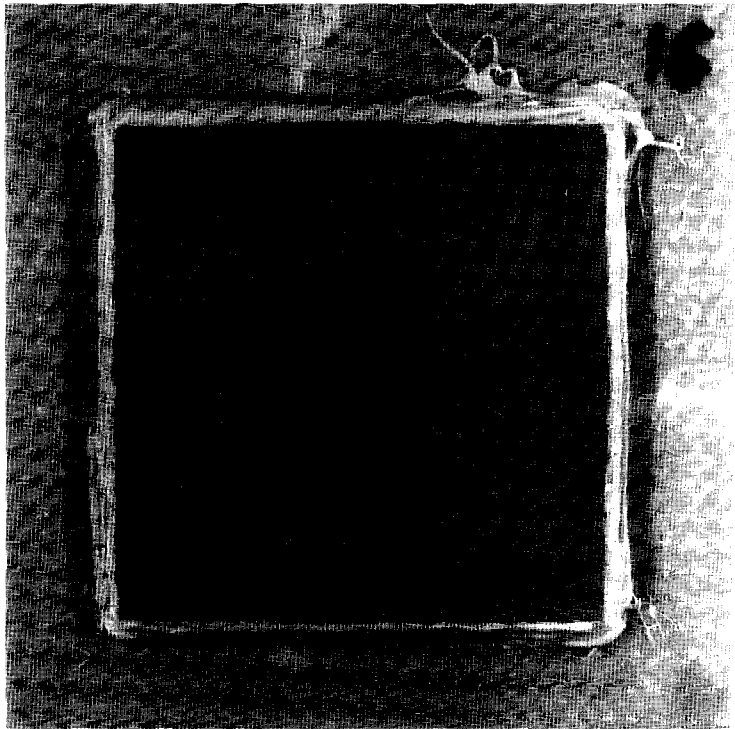


Fig. 6. Fracture geometry of a typical standard tile.

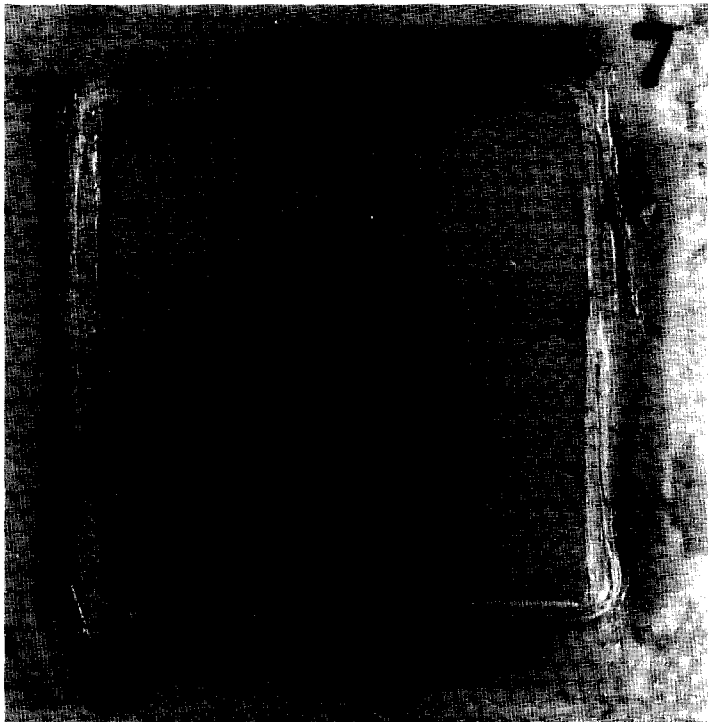


Fig. 7. Fracture geometry of a pre-cracked panel struck approximately 5 mm from the crack.

ascertain that the data was statistically significant. The Fisher F-test was applied to determine whether there was a significant difference in the variance. It was concluded that there was not sufficient evidence that the variance of the samples was different. The Student's t-test was then used to determine the significance of the difference in the mean velocities (the  $V_{50}$ ) of the standard and pre-cracked samples. This difference was determined to be

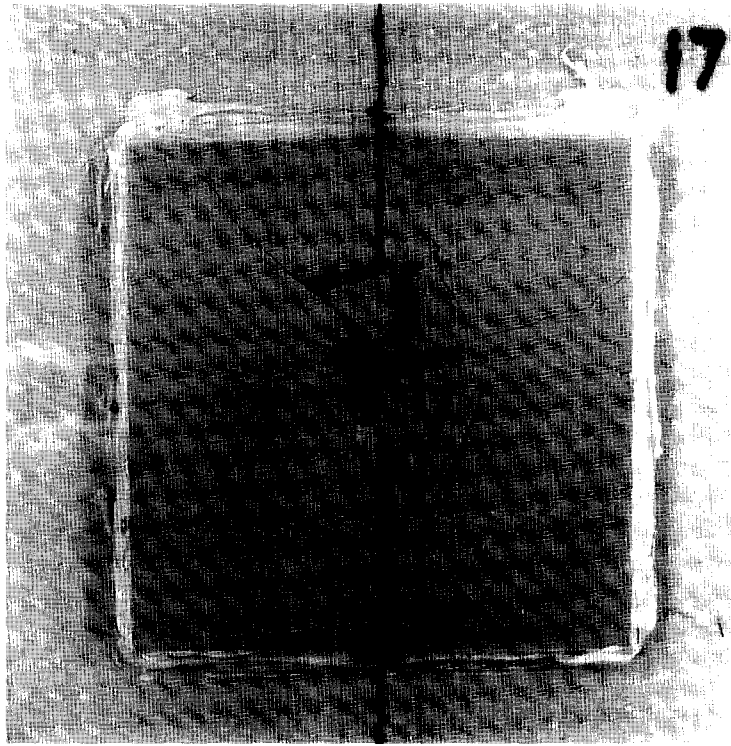


Fig. 8. Fracture geometry of a pre-cracked panel struck coincident with the crack. The target construction is shown diagrammatically in Fig. 2.

significant to a level of better than 1%. Therefore it is possible to conclude that the pre-crack does significantly reduce the  $V_{50}$  ballistic limit velocity.

An alternative measure of armour performance is to determine the highest velocity at which a projectile can strike with a negligible probability of penetration, the  $V_0$  ballistic limit velocity. It has been suggested [7] that the  $V_0$  ballistic limit velocity, may be a better measure of performance as it is more indicative in real terms of the ability of an armour to defeat a given threat and is a more readily understood concept to potential users. The  $V_0$  velocity can be calculated if the strike velocity  $V_s$  and residual velocity  $V_r$  are known:

$$V_0 = k(V_s^2 - V_r^2)^{1/2}. \quad (1)$$

The term  $k$  is used to correct for the actual residual projectile mass which may be reduced by erosion or supplemented by armour fragments. Therefore it is convenient to measure residual momentum using a ballistic pendulum rather than residual velocity. Although the  $V_0$  can be calculated from a single penetrating shot, it is more usual to use a graphical method as this gives a visual indication of experimental scatter.

Figures 4 and 5 show the data for the two target panel sets for which  $V_0$  has been calculated by a regression analysis using a linear fit for which error bars are shown. Residual momentum data has been shown to follow a curve defined by Eqn (1) [7], however a good approximation can be achieved with a linear fit given the relatively small interval between the  $V_0$  and the highest measured  $V_r$ . It is in any case not possible to fit a curve to the data as the value of  $k$  is not known and may vary as a function of impact velocity.

It must be noted that the  $V_0$  results are based upon relatively few data points and consequently their significance is limited. The pre-cracked panels have a  $V_0$  ballistic limit  $48 \text{ m s}^{-1}$  below that of the standard panels whilst the difference in the  $V_{50}$  is only  $24 \text{ m s}^{-1}$ . The greater the variability of the armour performance then the greater will be the difference between the  $V_{50}$  and  $V_0$ , this therefore has to be taken into account when comparing the two figures. However given the variability of the results it is doubtful whether much significance can be placed on the differences in the effect of the pre-crack on the measured  $V_0$  and  $V_{50}$ .



A major advantage of the  $V_0$  measure is that if the approximate shape of the residual momentum curve is known, then it is possible to estimate the ballistic limit from a single shot. This reduces the degree of hunting required to produce the requisite number and spread of velocities to calculate the  $V_{50}$ .

#### 4.2. Ballistic performance

In both sets of panels there is a degree of variability in performance such that the highest projectile velocity producing partial penetration was in both cases somewhat greater than the lowest velocity producing full penetration. However the data for the standard panels lies easily within the range allowed by the  $V_{50}$  test procedure. For the pre-cracked tiles the variability is greater, such that with the raw data the range of velocities is too great to allow a valid  $V_{50}$  to be calculated. This variability can be reduced by setting a limit on the aim error of approximately 1 projectile radius. Using data from only those impacts occurring 4 mm or less from the crack reduces the spread of data to within the acceptable range with only a slight change in the value of the ballistic limit velocity. The  $V_{50}$  ballistic limit calculated from 6 shots, for the standard and pre-cracked panels, is reduced from  $764 \text{ m s}^{-1}$  to  $740 \text{ m s}^{-1}$ . Using larger sample sizes to determine the  $V_{50}$  over 8 or 10 shots leads to only negligible changes in these values.

The drop in ballistic limit velocity of the pre-cracked panels is almost wholly due to a reduction in the average velocity of partially penetrating shots from  $772 \text{ m s}^{-1}$  to  $742 \text{ m s}^{-1}$ . The average velocity for full penetration is only reduced by a negligible amount from  $757 \text{ m s}^{-1}$  to  $756 \text{ m s}^{-1}$ . It would therefore appear that the effect of pre-crack is simply to increase the variability of the sample which produces a reduction in the measured  $V_{50}$ .

The method used to produce the pre-cracks in the panels ensured that the crack would remain closed. Consequently the material on the crack face is effectively constrained by the opposite crack face and experiences only slightly less constraint than material within the bulk of the panel. Under a ballistic impact the ceramic material is extensively comminuted and will undergo a volumetric expansion such that the effect of a pre-existing crack on this rubble will be suppressed. This situation should occur for any crack geometry which is effectively confined by the backing layer and spall shield, the only requirement being that the crack should not be able to open allowing a relief of the compressive stresses generated in the rubble. If cracks have only a marginal effect on ballistic performance then it follows reducing the resistance to cracking in the ceramic by reducing its tensile strength will not have a significant effect on ballistic performance. This is in agreement with the work of Woodward *et al.* [4] which showed that for penetrators which are deformed during impact, which is the case in the work, ballistic efficiency is not simply related to tensile strength.

The crack geometry observed in the pre-cracked tiles was almost identical to that observed in the standard panels providing that the point of impact was effectively coincident with the crack. This combined with the small reduction in ballistic limit velocity indicates that the pre-crack has little effect on the mechanisms of projectile defeat. Similarly the effect of allowing data from shots landing further from the pre-crack is simply to increase the range of the data with only a very marginal change in the absolute value.

## 5. CONCLUSIONS

A single through-thickness crack in the ceramic component of a composite armour system produces a small but statistically significant reduction in the ballistic performance. The effect of a crack is to reduce the constraint acting upon the ceramic rubble ahead of the penetrator. However for a ceramic tile which is well bonded to the backing and spall shield the reduction in this constraint is negligible. Consequently, it should not be necessary to replace a cracked armour panel which has been damaged in service, providing that the backing and spall shield preserve the structural integrity of the panel. This is of importance to the armour user as the environments in which ceramic armours may operate, such as on the outside of military vehicles, are such that some damage is inevitable.

The ballistic performance of such composite armour systems can be readily assessed by both  $V_{50}$  and  $V_0$  measures. The  $V_0$  measure is useful in its own right or can be used on unknown material to estimate the ballistic limit velocity and in so doing reduce the number of tests required to produce the data for the  $V_{50}$  measure.

*Acknowledgements*—The authors wish to thank Morgan Matroc Ltd and T&N Technology Ltd for providing target panel materials.

## REFERENCES

1. M. L. Wilkins, Mechanics of penetration and perforation. *Int. J. Engng Sci.* **16**, 793–807 (1978).
2. D. A. Shockey, A. H. Marchand, S. R. Skaggs, G. E. Cort, M. W. Burkett and R. Parker, Failure phenomenology of confined ceramic targets and impacting rods. *Int. J. Impact Engng* **9**, 263–275 (1990).
3. R. Cortes, C. Navarro, M. A. Martinez, J. Rodriguez and V. Sanchez-Galves, Numerical modelling of normal impact on ceramic composite armours. *Int. J. Impact Engng* **12**, 639–651 (1992).
4. R. L. Woodward, W. A. Gooch Jr, R. G. O'Donnel, W. J. Perciballi, B. J. Baxter and S. D. Pattie, A study of fragmentation in the ballistic impact of ceramics. *Int. J. Impact Engng* **15**, 605–618 (1993).
5. L. Baum, D. Sherman and D. G. Brandon, Ballistic failure process of constrained ceramic tiles. Presented Am. Cer. Soc. 1994 Annual Meeting, *Symp. on Performance of Ceramics Under Extreme Conditions*, Indianapolis (1994).
6. R. M. Ogorkiewicz, Advance in armour materials. *Int. Defence Rev.* **4**, July (1991).
7. L. B. Tobin, The evaluation of body armour and helmets: a reappraisal of the FSP  $V_0$  and  $V_{50}$  measures. SCRDE Research Report 93/2, Sept. (1993).
8. Stanag 2920 (draft), Edition 1, AC/301-D/378, NATO (1992).